S1 Table[1]: Antibody panels for flow cytometry

Antigen	Conjugate	Clone	Supplier
Panel 1			
CD3	ECD	UCHT1	Beckman-Coulter
CD4	Qdot605	S3.5	Invitrogen
CD8	APC-H7	SK1	BD
TCR-γδ	Brilliant Violet 421	B1	BD
CD56	Brilliant Violet 711	HCD56	BioLegend
IFNγ	AlexaFluor700	B27	BD
TNFα	PECy7	MAb11	eBioscience
IL-2	APC	MQ1-17H2	BD
IL-17	AlexaFluor488	N49-653	BD
IL-22	PE	IC7821P	R&D
Panel 2			
CD3	APC-H7	SK7	BD
CD8	Brilliant Violet 650	RPA-T8	BD
CD16	Brilliant Violet 510	3G8	BioLegend
CD26	APC	BA5b	BioLegend
CD56	Brilliant Violet 711	HCD56	BioLegend
CD57	Brilliant Violet 605	NK-1	BioLegend
CD66 (dump)	FITC	B1.1/CD66	BD
CD158b	PE	CH-L	BD
CD161	PECy5	DX12	BD
IFNγ	AlexaFluor700	B27	BD
TNFα	PECy7	MAb11	eBioscience
Perforin	Brilliant Violet 421	B-D48	BioLegend

[1] **S1 Table.** Antibody cocktails used in flow cytometry analysis of whole blood assays.

S1 Fig:

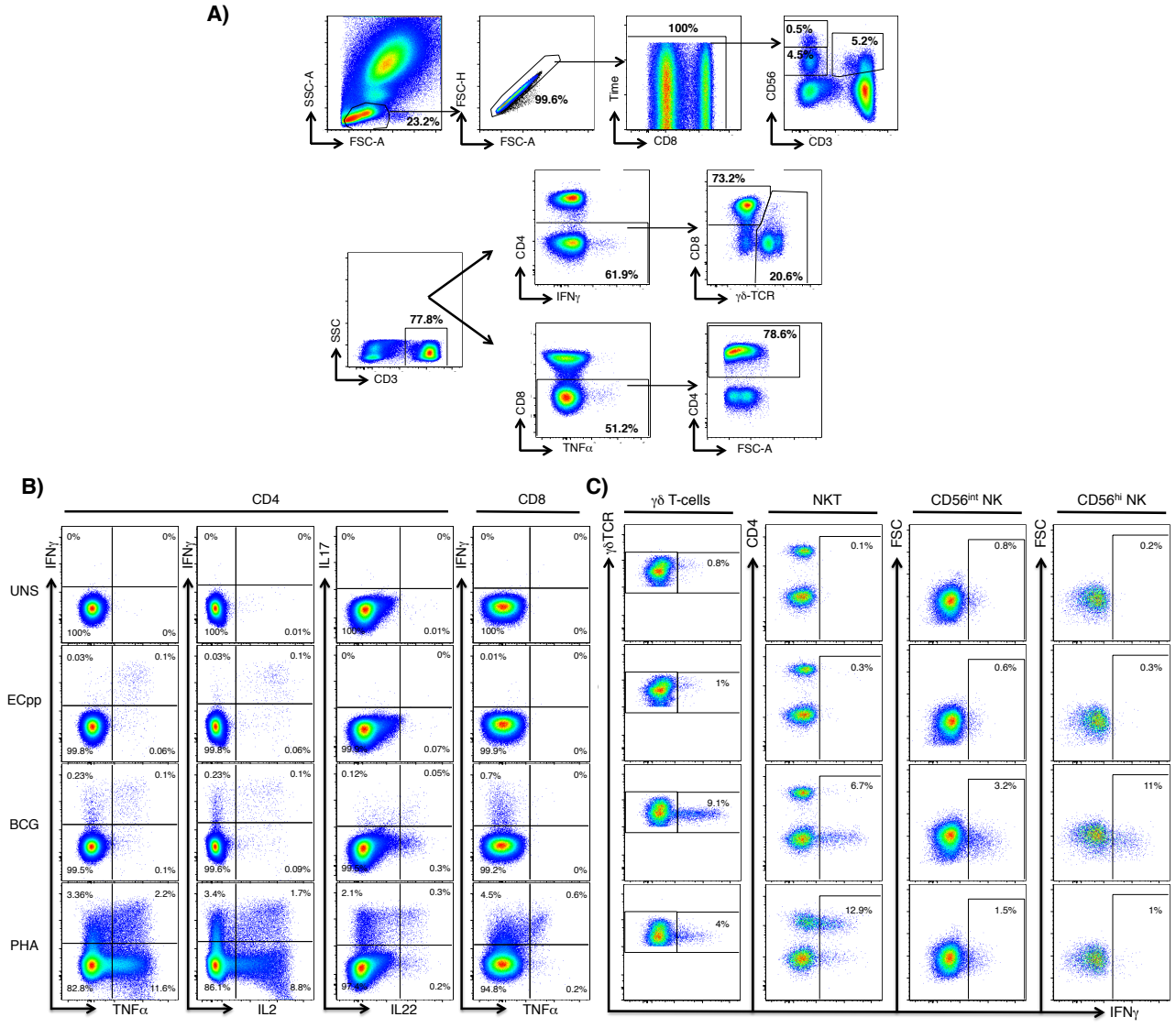

S1 Fig. Flow cytometry gating strategy: (A) Gating strategy applied to analyze stimulated whole blood samples. Small lymphocytes were gated based on forward (FSC) and side scatter (SSC), followed by doublet exclusion using FSC-area vs FSC-height. Then, to ensure uniform fluorescence during acquisition, a time gate was applied before identifying two $CD3^-$ natural killer (NK) cell subsets, defined as $CD56^{hi}$ and $CD56^{dim}$. From the time gate, we also identified γδ T and $CD8^+$ T cells amongst $CD3^+CD4^-$ cells (middle row) while $CD4^+$ T cells were identified amongst $CD3^+CD8^-$ cells (bottom row). **(B and C) Flow cytometric measurement of intracellular cytokine expression.** (**B**) Representative plots illustrating cytokine expression in $CD4^+$ and $CD8^+$ T cells from a single whole blood sample. Rows correspond to the four stimulation conditions used in the assay. (**C**) IFNγ-expression by γδ T cells, $CD3^+CD56^+$ NKT-like cells, $CD3^-CD56^{dim}$ NK and $CD3^-$ $CD56^{hi}$ NK cells.

S2 Fig:

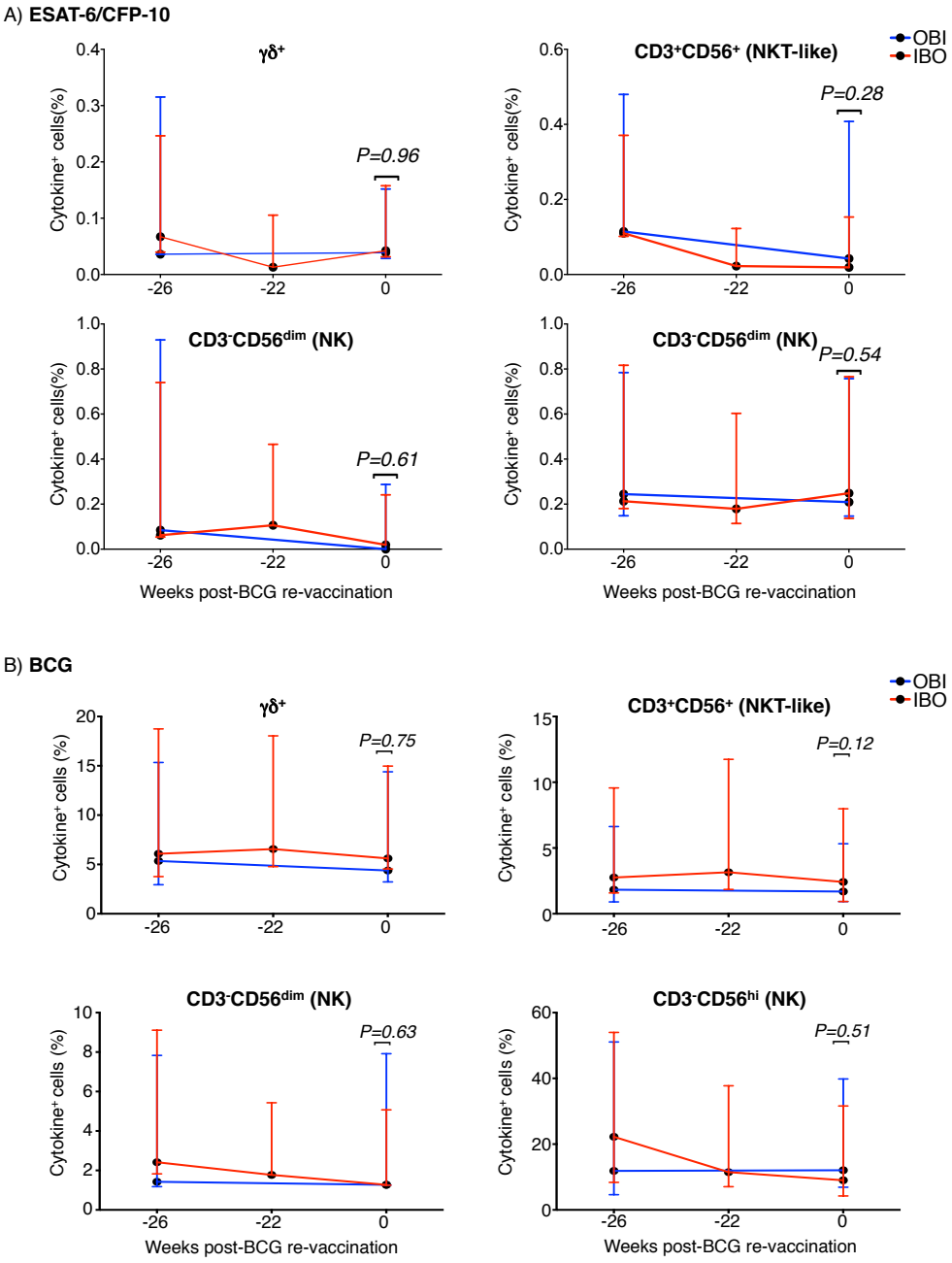

S2 Fig. Impact of INH treatment on antigen-specific responses to ESAT-6/CFP10 peptide pools (A) or BCG stimulation (B): Frequencies of antigen-reactive cytokine^{+} γδ (top left) T cells, CD3^{+}CD56^{+} NKT-like (top right), CD3^{-}CD56^{dim} NK (bottom left), and CD3^{-}CD56^{hi} NK (bottom right) cells. All frequencies were background subtracted. Red and blue lines correspond to group treated (IBO) or not treated (OBI) with INH for 6 months, respectively, in the time window preceding BCG re-vaccination. Unadjusted p-values were calculated with the Mann-Whitney *U*-test, comparing frequencies of cytokine-expressing cells between the two groups in each of the 6 immune subsets at the end of the 6-month INH Rx or observation. P-values below 0.025, correcting for testing in two groups using the Boneferroni method were considered statistically significant.

S3 Fig:

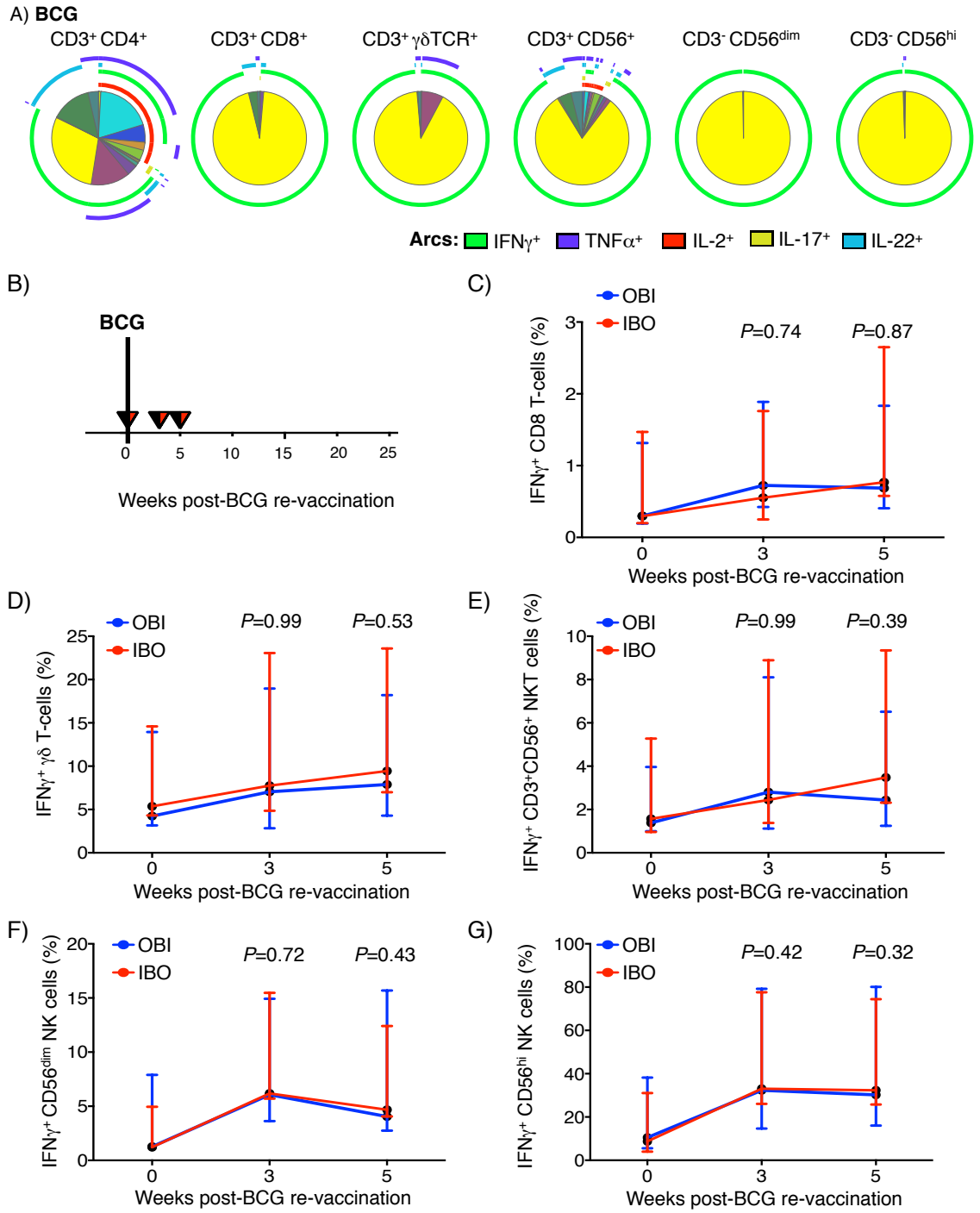

S3 Fig. Impact of INH pre-treatment on frequency of BCG-specific IFNγ production by non-CD4 T cells. (**A**) Pie charts showing median proportions of BCG-specific CD4, CD8, γδ T, $CD3^+CD56^+$ NKT-like, $CD3^-CD56^{dim}$ NK, and $CD3^-CD56^{hi}$ NK cells co-expressing IFNγ, TNFα, IL-2, IL-17, and/or IL-22 at 3 weeks post-vaccination. (**B**) Schematic diagram of blood draws to assess short-term boosting of BCG-specific responses. Median frequencies (error bars denote IQR) of IFNγ-expressing (**C**) CD8 T cells (defined as $CD3^+CD4^-CD8^+$ cells), (**D**) γδ T cells, (**E**) $CD3^+CD56^+$ NKT-like cells, (**F**) $CD3^-CD56^{dim}$ NK, and (**G**) $CD3^-CD56^{hi}$ NK cells. Unadjusted p-values, calculated with Mann-Whitney *U*-tests, represent inter-group comparisons.